First-Principle Time-Dependent Study of Magnesium-Containing Porphyrin-Like Compounds Potentially Useful for Their Application in Photodynamic Therapy

ARTICLE *in* THE JOURNAL OF PHYSICAL CHEMISTRY B · MAY 2008

Impact Factor: 3.3 · DOI: 10.1021/jp710880x · Source: PubMed

3 AUTHORS, INCLUDING:

Nino Russo
Università della Calabria
511 PUBLICATIONS **7,941** CITATIONS
SEE PROFILE

Emilia Sicilia
Università della Calabria
151 PUBLICATIONS **1,943** CITATIONS
SEE PROFILE

First-Principle Time-Dependent Study of Magnesium-Containing Porphyrin-Like Compounds Potentially Useful for Their Application in Photodynamic Therapy

Ida Lanzo, Nino Russo,* and Emilia Sicilia

Dipartimento di Chimica and Centro di Calcolo ad Alte Prestazioni per Elaborazioni Parallele e Distribuite-Centro d'Eccellenza MURST, Universita' della Calabria, I-87030 Arcavacata di Rende (CS), Italy

Received: December 4, 2007; In Final Form: January 15, 2008

Geometry optimization, singlet−triplet energy gap, and electronic absorption spectra calculation of complexes formed by Mg ion and porphyrin, porphyrazin, chlorine, bacteriochlorine, texaphyrin, phthalocyanine, naphthalocyanine, and anthracocyanine ligands have been carried out to elucidate their potentiality as photosensitizers in photodynamic therapy (PDT). The study has been performed employing the density functional theory (DFT) and its time-dependent approach (TDDFT) in conjunction with the PBE0 exchange-correlation functional and extended TZVP all-electron basis sets. The solvent effects have been evaluated throughout the polarizable continuum model (PCM). Results show that, following the properties requirement for the drugs used in PDT, the Mg−Tex and Mg−Pc complexes are reliable candidates for their use as photosensitizers in this medical therapy.

1. Introduction

In these last years the interest in proposing new compounds for their use as photosensitizers in photodynamic therapy (PDT) is rapidly growing due to the possible extension of this noninvasive therapy in many kinds of human diseases.[1−4] In fact, these days this mode of disease treatment not only accounts for the therapy of a variety of cancer types but is currently being explored in the areas of cardiology, ophthalmology, dermatology, immunology, genecology, and urology.[5−8] In addition, PDT is becoming a potential alternative to the antimicrobial agent in the inactivation of many microbial infections.[9]

The working mechanism of PDT can be summarized as follows: (i) A nontoxic photosensitizer is introduced in the body of the appropriate target. (ii) The target is irradiated with light of appropriate wavelength, ranging from 600 to 900 nm (the so-called therapeutic window), in order to excite the photosensitizer in its ground state (S_0) to a shorter-lived first excited state (S_1). (iii) S_1 can undergo conversion to the first excited triplet state (T_3) by intersystem crossing. Then the T_3 state of the sensitizer can release its energy to the surrounding biological tissue exciting the O_2 from its triplet to the highly reactive singlet state (O_1) that induces an oxidative cellular damage leading to the apoptosis or necrosis of the cells. (iv) Finally, the photosensitizer returns to its ground state and the cycle can be repeated with a new light irradiation. At the end of the therapeutic cycle the sensitizer is eliminated from the body.

In the last 10 years different generations of new synthesized molecules have been proposed as photosensitizers for PDT.[10−14] Many of them are porphyrin-like systems, but also a new class of non-porphyrin PDT agents based on the tetrarylazadipyrromethenes group has been synthesized, characterized, and tested at the biological level.[15,16]

A number of these compounds are in an advanced stage of clinical testing or already used in the treatment of various diseases (i.e., various solid tumors, macular degeneration) for which PDT was proved to be effective.

In the rational design of a new photosensitizer active in PDT the following factors should be taken into consideration:[17]

(1) The core of the system, generally a ligand, should be represented by a moiety able to absorb in the therapeutic window (600−900 nm) and preferably should be red-shifted. It is well-known, indeed, that high absorbance values increase the penetration efficiency in the biological tissue (i.e., a 500 nm wavelength radiation penetrates into the tissue for about 3.5 mm, whereas the depth of light penetration reduces to about 8 mm at 700 nm). This requirement can be achieved also by adding appropriate substituents around the ligand.

(2) The presence of a metal or a heavy atom generally increases the efficiency of the singlet−triplet intercrossing (the so-called heavy atom effect) due to the enhanced spin−orbit perturbations.

(3) The energy gap between singlet and triplet states should be higher than the energy required to excite the oxygen molecule in its singlet state (about 1 eV). In addition, the triplet state should be generated with high quantum yield ($\varphi > 0.4$) and lifetimes ($>1\ \mu$s).

(4) The photosensitizer should have a high photo- and thermodynamic stability. A good photosensitizer should be a single substance with constant composition and a high degree of chemical purity and sufficiently stable under physiological conditions. Empirical studies based on the stability index,[18] $Si = 100\chi(Z/ri)$ (where χ = Pauling electronegativity, Z = oxidation number, ri = effective ionic radius of a central metal ion), show that in the case of porphyrin-like molecules the stability order is phthalocyanines > phorphyrins > chlorines. In the case of their complexes with transition metals the stability order is Ru(III), Al(III), Sn(IV) > Mg(II), Cd(II).

(5) The photosensitizer should have no toxicity in the dark.

The aim of present paper is the prediction and characterization, especially in the Q-band region, of a series of porphyrin-like systems with different numbers of π electrons, namely, porphyrin (P), porphyrazin (Pz), chlorine (C), bacteriochlorine (BC), texaphyrin (Tex), phthalocyanine (Pc), naphthalocyanine (Nc), and anthracocyanine (Ac), and their complexes with magnesium cation, by using the time-dependent extension of density functional theory (TDDFT). This method has been

10.1021/jp710880x CCC: $40.75
Published on Web 03/07/2008

TABLE 1: Electronic Transition Energies (in eV and nm) for the Free Ligands Pc, Nc, and Ac Obtained by TDDFT at PBE0 Optimized Geometries

	vacuum				solution			
state	excitation energy	*f*	main configuration	excitation energy	ass.	gas phase[a]	*tert*-butyl pyridine[b]	1Cl-naph[a]
				Pc				
B_{1u}	2.10 (590)	0.430	92% (0−1)	2.09 (590)	Q_x	1.81 (686)	1.79 (698)	1.79 (698)
B_{2u}	2.12 (585)	0.479	94% (0−0)	2.10 (589)	Q_y	1.99 (623)	1.87 (664)	1.87 (663)
				Nc				
B_{2u}	1.77 (702)	0.658	97% (0−0)	1.75 (707)	Q_x		1.58 (784)	
B_{3u}	1.84 (673)	0.642	95% (0−1)	1.83 (675)	Q_y		1.66 (747)	
				Ac				
B_{2u}	1.49 (830)	0.698	98% (0−0)	1.48 (833)	Q_x		1.45 (854)	
B_{3u}	1.65 (752)	0.764	97% (0−1)	1.63 (758)	Q_y		1.53 (810)	

[a] From ref 38. [b] From ref 39.

TABLE 2: Total (hartrees) and Relative (eV) Energies for All the Considered Complexes

molecule	state	*E* (hartree)	ΔE (eV)	ΔE_{solv} (eV)[a]
Mg−BC	^1A_g	−1190.036641	0	0
	$^3B_{2u}$	−1190.008021	0.78	0.79
Mg−C	^1A_g	−1188.838145	0	0
	$^3B_2$	−1188.784919	1.44	1.45
Mg−P	^1A_g	−1187.631863	0	0
	^3E_u	−1187.571884	1.63	1.62
Mg−Pz	^1A_g	−1251.748181	0	0
	^3E_u	−1251.697381	1.38	1.39
Mg−Tex	^1A_g	−1941.119191	0	0
	^3B	−1941.080638	1.04	1.05
Mg−Pc	^1A_g	−1865.832939	0	0
	^3E_u	−1865.795254	1.02	1.03
Mg−Nc	^1A_g	−2479.860282	0	0
	^3E_u	−2479.830865	0.80	0.81
Mg−Ac	^1A_g	−3093.865208	0	0
	^3E_u	−3093.841505	0.64	0.65

[a] Chloronaphthalene.

successfully used for the calculation of excitation energies and oscillator strengths in a variety of molecular systems[19−23] including porphyrin-like systems and their metal complexes.[19,20]

The choice to study the magnesium complexes of the ligands listed above is essentially due to the following reasons:

(1) Mg cation is one of the essential metals in many biological processes and does not present any kind of cytotoxicity.

(2) The coordination of Mg cation to some porphyrin-like ligands has been previously studied, and some controversial results on its effect on the absorption spectra have been reported. In fact, in some cases[24,25] it was found that the presence of Mg-(II) increases the absorption coefficient of the Q_x band, whereas in another study[26] it was reported that the Mg coordination affects only the symmetric degeneracy of the absorption but not the intensity of the Q_x band.

(3) To our knowledge no indication on their potential use in PDT exists until now.

2. Method

Full geometry optimization for each studied free ligand and corresponding magnesium complex has been carried out using the Turbomole program[27] employing the PBE0[28] exchange-correlation functional and the TZVP all-electron basis set.[29] This functional, based on the generalized gradient functional PBE[30] with 25% exact exchange, has been chosen as it generally reproduces geometrical parameters, also in metal-containing systems, within experimental error.[28] As recently shown,[19,20] it is also able to correctly predict the absorption spectra and the oscillator strengths in a series of porphyrin-like ligands and in their metal complexes. The nature of the minima has been verified by computing vibrational modes, and no imaginary frequency has been calculated for any of the systems under investigation. The use of TZVP-quality basis sets ensures the convergence on the electronic spectra as recently demonstrated in a series of papers.[19−23,29,31] Absorption spectra have been computed as vertical excitations from the ground-state minima structures by using the TDDFT approach as implemented in Turbomole code.[27,29,31]

Solvent shifts of the excitation bands have been evaluated using the conductor-like approach (Cosmo[32]) within the framework of the polarizable continuum method (PCM)[33,34] as implemented in the Turbomole code. Since the available experimental absorption spectra have been recorded in solvents with low polarity (chloronaphthalene), the use of explicit solvent molecules can be avoided, while PCM is able in these cases to provide reliable results. The solvatochromic shifts have been calculated by using optimized gas-phase geometries.

TABLE 3: Distances (angstroms) of the Metal−Nitrogen Bond for the Studied Complexes

compounds	symmetry	d_{Mg-N}	d_{Mg-N1}	d_{Mg-N2}	exptl
Mg−BC	D_{2h}	2.124	2.040		
Mg−C	C_{2v}	2.111	2.047	2.060	
Mg−P	D_{4h}	2.053			2.071[a]
Mg−Pz	D_{4h}	1.974			
Mg−Tex	C_2	2.158	2.245	2.604	
Mg−Pc	D_{4h}	1.998			2.017−2.030[b]
Mg−Nc	D_{4h}	2.005			
Mg−Ac	D_{4h}	2.008			

[a] From ref 40. [b] From ref 41.

3. Results and Discussion

3.1. Excited States of Free Ligands. Before discussing the results for the magnesium-containing complexes we analyze the structures and absorption spectra of the free ligands. Some of them have been previously studied using several theoretical methods including that used here,[22,35−38] so we report our result

SCHEME 1

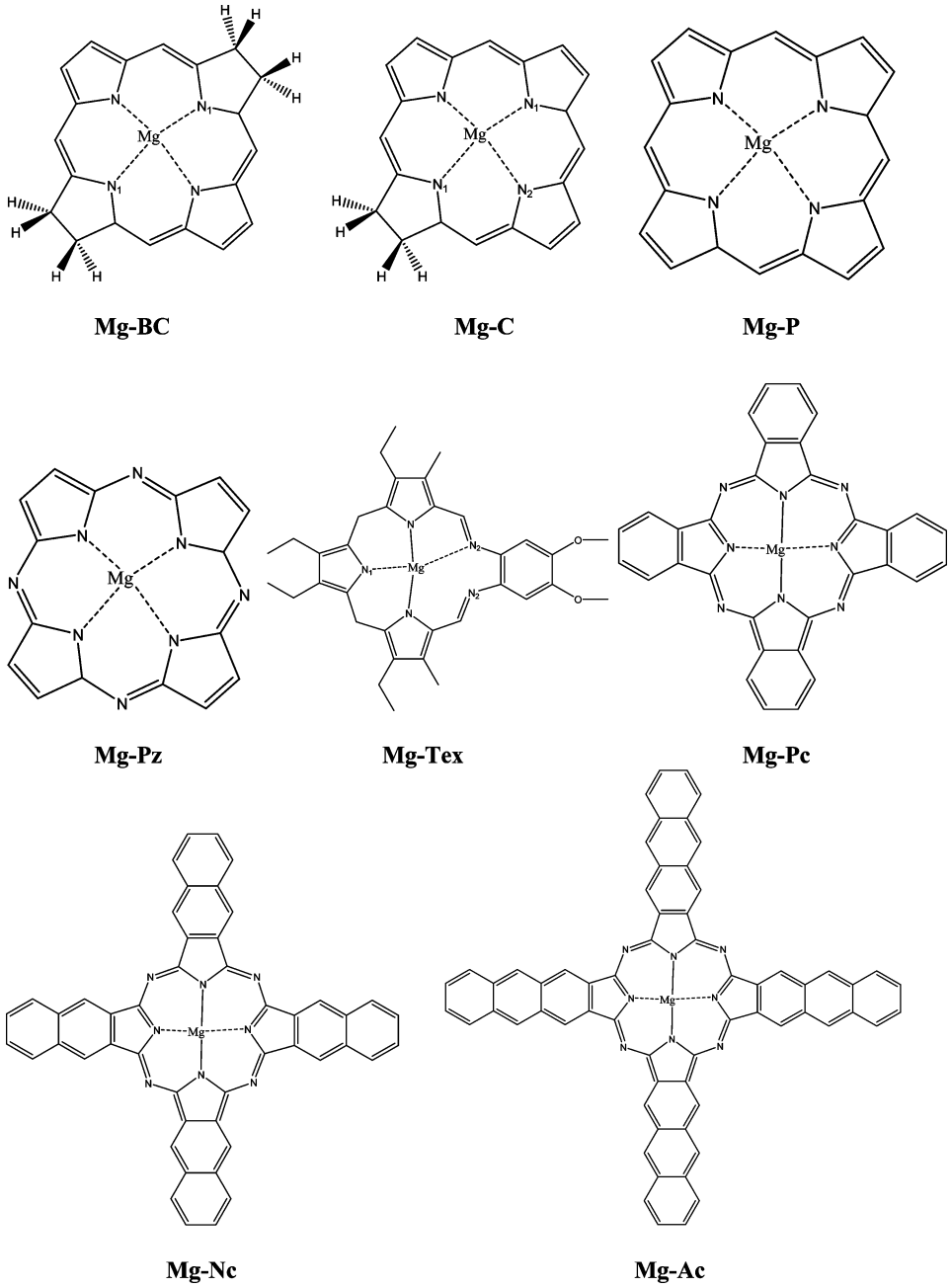

for the Pc, Nc, and Ac systems for which previous theoretical studies do not exist or the available data have been obtained by different theoretical methods. Previous experimental data concern the Pc, for which both gas-phase and solution[38] (chloronaphthalene solvent) absorption spectra are known. In a more recent study the tetra-*tert*-butylated species of Pc, Nc, and Ac have been studied in solvent by Kobayashi et al.[39] Our results together with experimental data are collected in Table 1. As can be inferred from this table, our values for the Q-band are satisfactorily reproduced the difference between theoretical and experimental spectra being about 0.2 eV. In particular, the theoretical Q-band values result to be blue-shifted with respect to the experimental measurements. In a previous theoretical work performed by using the symmetry-adapted cluster-configuration interaction method (SAC-CI) the discrepancy between the computed and experimental Pc absorption spectra is about 0.5 eV in the Q-band region.[37] Starting from Pc, the annulation of further benzene rings at the Pc moiety increases the number of π electrons and the HOMO−LUMO gap decreases (2.35, 1.97, and 1.72 eV for Pc, Nc, and Ac, respectively). Consequently, the Q-band sensibly shifts to longer wavelength (see Table 1). This behavior is in good agreement with recent half-wave redox potentials measurement for Pc (^{t}Bu)$_4$ and Nc(^{t}Bu)$_4$(Y).[38] Our computed H−L energy gap decreases in going from Pc to Nc by 0.38 eV, whereas the experimental counterpart for the *tert*-butyl derivatives is 0.25 eV.[38] Since we are interested in possible application of these compounds in the PDT it is worth it to note that the value of the oscillator strength for the Q-band increases with the enlargement of the π system. The decrease in the HOMO−LUMO gap is almost determined by the destabilization of the HOMO as one goes from Pc (5.42 eV) to Nc (4.97 eV) and Ac (4.71 eV). The next occupied orbital (next-HOMO) follows the same behavior. The LUMO orbital energy does not change significantly and retains its value of about 3 eV along the series, whereas the next unoccupied orbital (next-LUMO) is significantly stabilized in going from Pc to

TABLE 4: Excitation Energies (eV and nm), Oscillators Strengths, Configurations, and Experimental and Previous Theoretical Data for the Studied Mg Complexes[a]

	vacuum			solution			
state	excitation energy	*f*	main configuration[b]	excitation energy	*f*	exptl	theory
			Mg−BC				
$^1B_{2u}$	2.03 (610)	0.282	93.1% (0−0)	2.03 (609)	0.286	2.06[c,d]	1.79[e] 2.05[f]
$^1B_{3u}$	2.53 (490)	0.045	71.4% (1−0) + 27.6% (0−1)	2.53 (490)	0.054		1.90[e]
			Mg−C				
$^1B_2$	2.36 (525)	0.129	80% (0−0) + 18.8% (1−1)	2.36 (525)	0.120	2.03[g]	1.95[e]
$^1A_1$	2.54 (488)	0.003	59.5% (1−0) + 39.5% (0−1)	2.52 (488)	0.005	2.15[g]	2.32[e]
			Mg−P				
^1E_u	2.43 (509)	0.001	51.5% (0−0) + 47.7% (1−0)	2.43 (509)	0.001	2.30[h]	2.21[i] 2.14[j] 2.23[k]
			Mg−Pz				
^1E_u	2.49 (499)	0.332	81.2% (0−0) + 17.8% (1−0)	2.48 (499)	0.332	2.34[l]	2.08[l]
			Mg−Tex				
^1B	1.95 (626)	0.083	83.7% (0−0) + 14.7% (1−1)	1.98 (626)	0.091		
^1A	2.07 (596)	0.082	69.1% (1−0) + 29.4% (0−1)	2.08 (596)	0.086		
			Mg−Pc				
^1E_u	2.10 (590)	0.915	93.4% (0−0)	2.10 (590)	0.936	1.82[m]	
			Mg−Nc				
^1E_u	1.80 (688)	1.307	96.5% (0−0)	1.80 (688)	1.337	1.84[n,o]	
			Mg−Ac				
^1E_u	1.57 (789)	1.408	97.3% (0−0)	1.29 (789)	1.219		

[a] Experimental spectra are referred to the chloronaphthalene solvent. [b] In parenthesis are reported the orbital contributions with the convention that the first number, *n*, refers to the occupied orbitals (HOMO − *n*), and the second (*m*) to the virtuals (LUMO + *m*). [c] From ref 42. [d] From ref 43. [e] From ref 50. [f] From ref 51. [g] From ref 44. [h] From ref 45. [i] From ref 52. [j] From ref 26. [k] From ref 53. [l] From ref 49. [m] From ref 46. [n] From ref 47. [o] From ref 48.

Nc and Ac. Adding the solvent effects through the PCM tool we note that the Q-bands are not affected by the presence of the solvent, the maximum shift being about 0.02 eV. In the case of Pc, for which are available absorption spectra both in gas phase and in solvent,[38,39] we can verify that our prediction is correct. This behavior can be understood if we consider the low polarity of the solvents. From Table 1 it is evident that along the series the Q_x band is essentially due to the HOMO → LUMO transition (more than 90%) with a small contribution coming from next-HOMO → next-LUMO. The Q_y counterpart is mainly originated by a HOMO → next-LUMO transition (more than 90%), and only a very small contribution stems from the next-HOMO → LUMO excitation. Finally, we have computed the energy gap between the ground singlet and low-lying triplet excited states (ΔE_{S-T}) for these ligands. Pc has the larger ΔE_{S-T} value (0.91 eV) followed by Nc (0.63 eV) and Ac (0.42 eV). This behavior follows, as expected, that of the HOMO−LUMO gap in the series. On the basis of this result we can predict that for the possible PDT applications the best photosensitizer is Pc that has an energy gap close to that needed to excite molecular oxygen to its singlet state.

3.2. Ground-State Properties of Mg(II) Complexes. The studied complexes have been optimized by using the proper symmetry constraint and considering both the singlet and triplet spin states. Table 2 collects all these results. In all cases, the singlet configurations are more stable than the triplet ones. Always we find a planar geometry around the metal center. The Mg−N bond distances are reported in Table 3. Owing to the chemical and structural similarities, all the compounds except the Mg−Tex complex have similar Mg−N bond lengths that range from 1.974 Å for Mg−Pz to 2.124 Å for Mg−BC. A comparison between computed and experimental geometries is possible only for the Mg−P and Mg−Pc systems for which X-ray structures are available.[40,41] Our Mg−N bond distance in the Mg−P complex is 2.053 Å, whereas the experimental counterparts is 2.071 Å.[40] A larger error is found in the case of Mg−Pc in which the computed Mg−N distance (1.998 Å) appears to be slightly shorter than the corresponding X-ray value.[41] In any case the difference between the two values is only 0.019 Å. In the Mg−Tex complex, in which the cavity is larger with respect to the other considered magnesium complexes, it is evident that the main interaction occurs between magnesium and pyrrolic nitrogens in a three-coordinated fashion. The distance of the metal from the N_2 atoms (see Scheme 1) is longer (2.604 Å). In some complexes of the texaphyrin ligand with transition metal atoms, the available X-ray structures demonstrate that this coordination mode has already been found.[20] In order to verify whether the imposed symmetry constraints might have consequences on the obtained structures, we have fully reoptimized Mg−C, Mg−Pz, and Mg−Pc geometries without symmetry constraints. The results show that geometrical parameters as well as energetic ones do not change

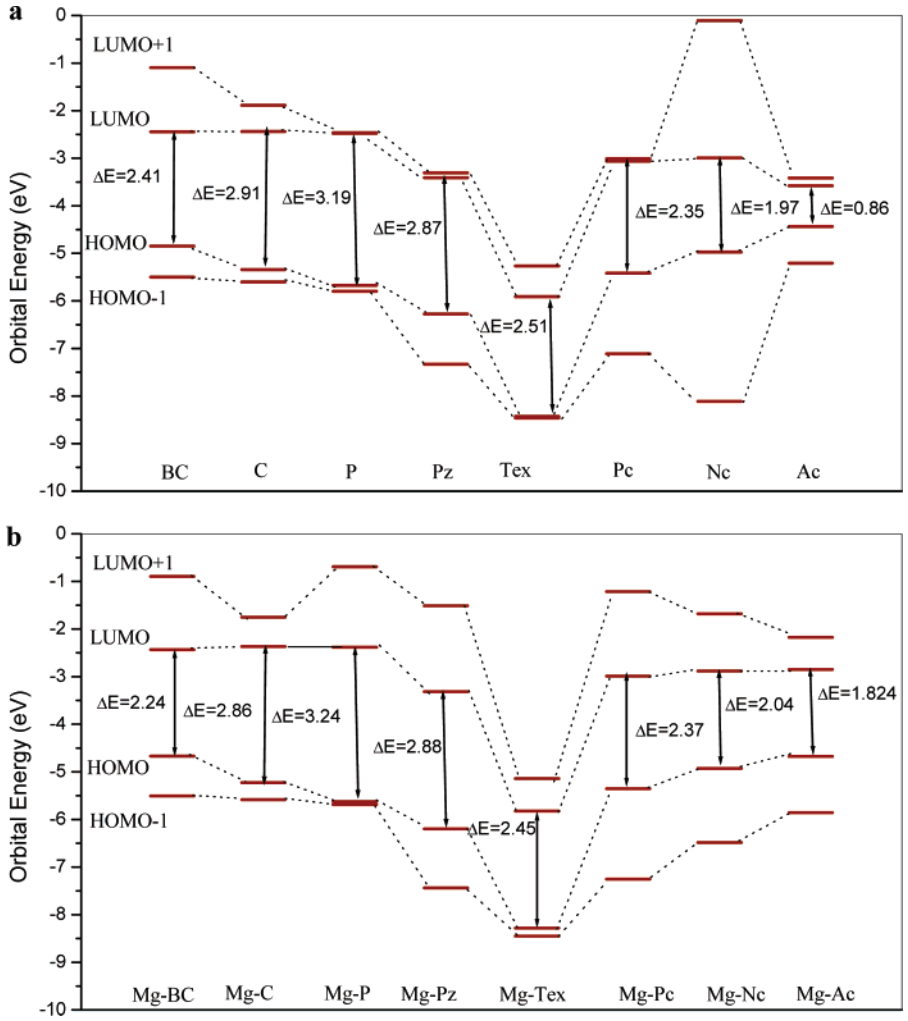

Figure 1. Orbital energy levels of the Gouterman orbitals for free bases (a) and the considered complexes (b).

in these circumstances. Similar evidence has been previously reported for first-row transition metal bacteriochlorine and texaphyrin complexes.[19,20]

Concerning the energy gap between singlet ground state and excited triplet state (ΔE_{S-T}) we note that the values range from 0.64 (Mg−Ac) to 1.63 (Mg−P) eV. These calculations are important since this property is crucial in the working mechanism of PDT. From the data reported by us it is possible to infer that all the complexes, except Mg−Ac, Mg−Nc, and Mg−BC, exhibit a ΔE_{S-T} greater than 1 eV and can excite the molecular oxygen from its singlet to triplet electronic state. This means that Mg−C, Mg−P, Mg−Pz, Mg−Tex, and Mg−P possess one of the main requirements to be proposed as photosensitizers in PDT. This parameter has been estimated also in solvent performing a single-point PCM computation on the in vacuo optimized geometries of both singlet and triplet states. As shown in Table 2, the presence of the solvent (chloronaphthalene $\epsilon = 5.0$) does not change gas-phase values.

3.3. Excited States of Mg Complexes. As previously mentioned, the activity of the photosensitizers in PDT is closely related to their spectral features and in particular to the absorption energies in the so-called Q-band. For this reason we carefully discuss the excitation energies that fall in the Q-band. Results are collected in Table 4 together with the available experimental data[42−49] and previous theoretical computations.[26,51−53] As a first step we discuss the computed Q-band for Mg−BC, Mg−C, and Mg−P for which are available both experimental data and previous theoretical computations performed at different levels of theory. The Q_x and Q_y components for Mg−BC are found to be at 2.03 and 2.53 eV, respectively. The experimental value in solvent is 2.06 eV[42,43] for the more intense Q_x component. Previous TD-B3LYP computations give values of 1.79 and 1.90 eV for Q_x and Q_y, respectively,[50] whereas another similar computation, performed at HF and B3LYP levels, gives 2.05 eV for the Q_x component.[51] The composition of the Q_x transition is mainly due to the HOMO−LUMO transition (93.1%), whereas in the Q_y component the next-HOMO → LUMO transition is dominant with a contribution from the HOMO → next-LUMO (about 27%). The Q_x and Q_y components of the Q-band of Mg−C are found to fall at 2.36 and 2.54 eV, respectively, the first one being much more intense. The experimental counterparts are 2.03 and 2.15 eV, respectively, whereas at the B3LYP level of theory the predicted values are 1.95 (Q_x) and 2.32 eV (Q_y). In this case the Q_x component is again more intense than the corresponding Q_y one, and the orbitals involved in the transitions are (HOMO → LUMO) (80%) and (next-HOMO → next-LUMO) (18.8%) for Q_x and (next-HOMO → LUMO) (59.5%) and (HOMO → next-LUMO) (39.5%) for Q_y. In the case of the Mg−P complex only one component of the Q-band is observed in agreement with the experimental evidence[45] and previous theoretical computations.[53] The predicted PBE0 value is 2.43 eV in good agreement with the experimental value (2.30 eV). Our study, according to previous theoretical computations, predicts a low intensity for this excitation energy that is equally composed of HOMO → LUMO and next-HOMO → LUMO transitions. Also for the

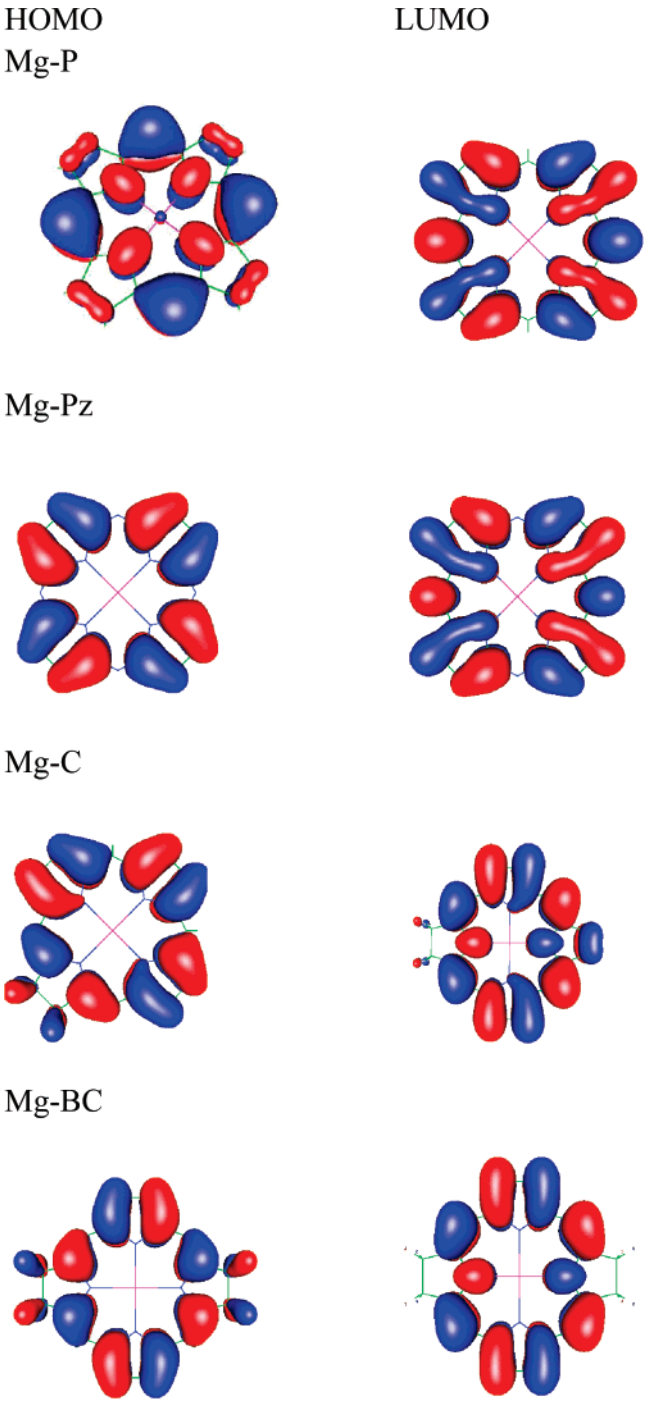

Figure 2. Plot of the HOMO and LUMO orbitals for Mg−P, Mg−Pz, Mg−C, and Mg−BC complexes.

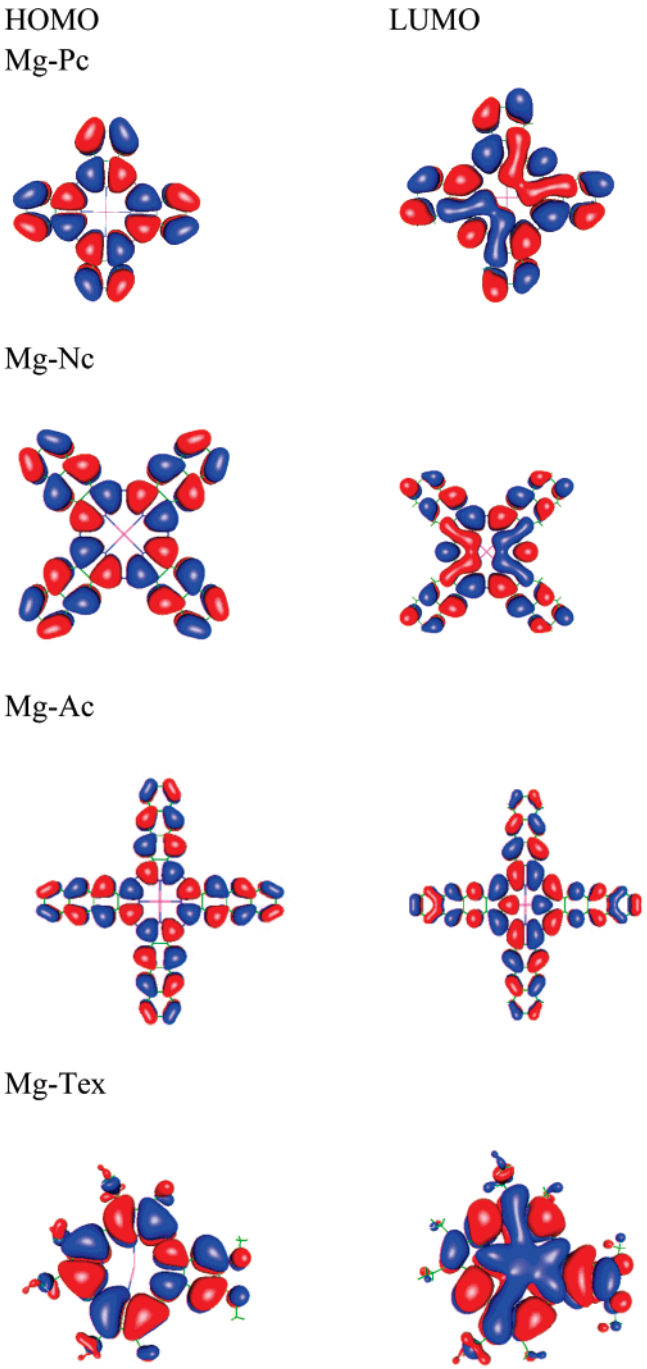

Figure 3. Plot of the HOMO and LUMO orbitals for Mg−Pc, Mg−Nc, Mg−Ac, and Mg−Tex complexes.

Mg−Pz system we find a single value at 2.49 eV for the Q-band, and the agreement with the experiment is quite good (2.48 vs 2.34 eV). The value of the oscillator strength indicates an intense band that mainly arises from HOMO → LUMO (81.2%) and next-HOMO → LUMO (17.8%) transitions. The Mg−Tex complex shows Q_x and Q_y transitions at 1.95 and 2.07 eV, respectively, with low intensity (in both cases the value of the oscillator strength is about 0.08 eV). The most important component of the Q_x transition is the HOMO → LUMO (83.7%), whereas for the Q_y it is the HOMO → next-LUMO) (69.1%). Finally, for the Mg−Pc, Mg−Nc, and Mg−Ac it is worth it to underline the presence of an only intense transition at 2.10, 1.80, and 1.57 eV, respectively, in the Q region. In order to rationalize these behaviors, we have examined the four Gouterman orbitals for all the considered compounds. In Figure 1 are reported the energies for the frontier orbitals of both the free ligands and the corresponding complexes. In going from Mg−BC to Mg−Pz the obtained values for the Q transitions do not follow the trends of the HOMO−LUMO gap essentially why the transitions in the different compounds do not involve only the HOMO → LUMO transition, but significant contributions come also from the next-HOMO and next-LUMO orbitals. Figure 1b clearly shows that these orbital energies, above all that of the next-LUMO, change significantly in going from Mg−BC to Mg−Pz complexes. As expected, the Mg−Tex system has different Gouterman orbital energies with respect to the other examined complexes. The reason could be that the ring of the texaphyrin ligand is expanded with respect to those of the other ligands. The behavior of the excitation energies found for the

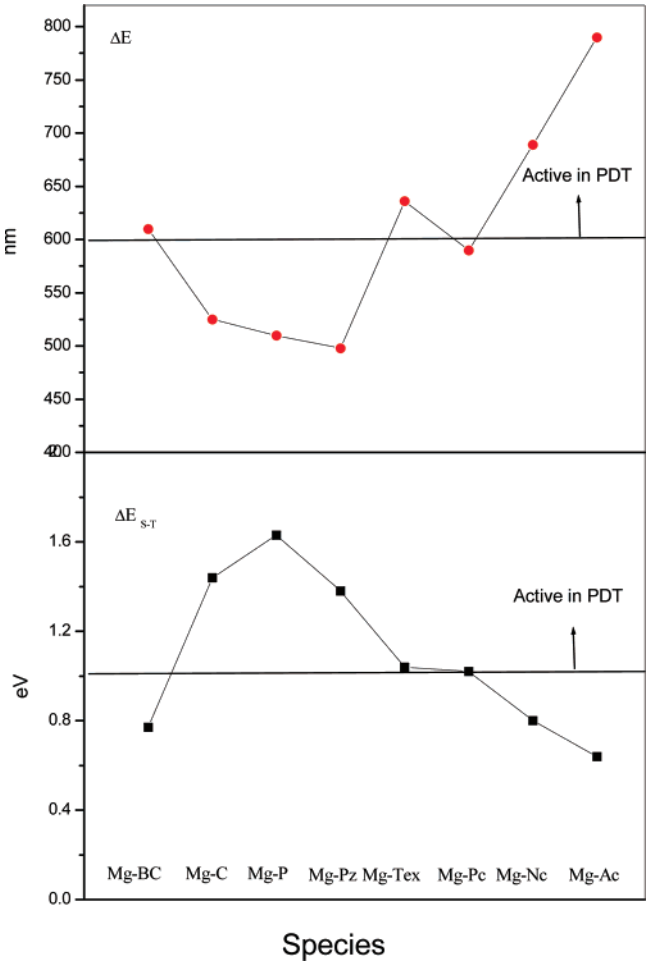

Figure 4. Plot of the Q-band and ΔE_{S-T} values for the considered complexes.

last three complexes (Mg−Pc, Mg−Nc, and Mg−Ac) follows that of the HOMO−LUMO gap since the Q-band is characterized by the presence of only the HOMO → LUMO transition. The molecular orbital wave functions for the four Gouterman orbitals of the studied systems are depicted in Figures 2 and 3. From these figures it is evident that the frontier orbitals show π characters distributed over the whole molecules, although the largest contributions come from the chromophore moiety. The HOMO possesses bonding character, and the LUMO is essentially antibonding in nature. Furthermore, the contribution of the metal is negligible in all cases.

From an inspection of Table 4 it is evident that the introduction of the solvent effects through the PCM does not affect significantly the results obtained in vacuum conditions basically because of the low polarity of the solvent in which the experimental spectra have been registered.

When the results concerning the wavelengths of the Q transitions and the results obtained for the energy ΔE_{S-T} separations are looked at, some indications about the possible use of these complexes in PDT can be outlined. Figure 4 collects the results concerning these two parameters. The systems that show the absorption Q-bands in the therapeutic window (600−900 nm) are Mg−Tex, Mg−Pc, Mg−Nc, and Mg−Ac. On the other hand, the only systems that present a ΔE_{S-T} gap lower than the corresponding value for dioxygen are the Mg−Nc, Mg−Ac, and Mg−BC complexes for which our computed value are 0.80, 0.65, and 0.78 eV, respectively. Combining these two parameters we can predict that among the studied systems, the best candidates for their use in PDT should be, in order of preference, Mg−Tex and Mg−Pc molecules.

Conclusions

Time-dependent density functional computations have been performed on the excited states of a series of magnesium(II) complexes with porphyrin, porphyrazin, chlorine, bacteriochlorine, texaphyrin, phthalocyanine, naphthalocyanine, and anthracocyanine ligands. Special emphasis has been devoted to the reproduction and prediction of the Q-bands and to the singlet−triplet energy gap in view of the possible use of these systems as photosensitizers in PDT. On the basis of our study the following conclusions can be drawn:

(1) The employed method gives results that are in reasonable agreement with the experimental spectra.

(2) The only magnesium complexes that show transitions in the range of the PDT therapeutic window (600−900 nm) are those containing the texaphyrin, phthalocyanine, naphthalocyanine, and anthracocyanine ligands.

(3) Mg−C, Mg−P, Mg−Pz, Mg−Tex, and Mg−Pc possess singlet−triplet energy gaps equal or larger than the corresponding energy difference in oxygen molecule.

From these computed properties we can conclude that only the Mg−Tex and Mg−Pc complexes can be indicated as good candidates for their use as photosensitizers in PDT.

Acknowledgment. The authors thank the MIUR and the Università della Calabria for the financial support.

References and Notes

(1) MacDonald, I. J.; Dougherty, T. J. *J. Porphyrins Phthalocyanines* **2001**, *5*, 105−129.
(2) Van Tenten, Y.; Schuitmaker, H. J.; De Wolf, A.; Willekens, B.; Vrensen, G. F. J. M.; Tassignon, M. J. *Exp. Eye Res.* **2001**, *72*, 41−48.
(3) Dolmans, D. E. J. G. J; Fukumura, D.; Jain, R. K. *Nat. Rev. Cancer* **2003**, *3*, 380.
(4) Dougherty, T. J.; Gomer, C. J.; Henderson, B. W.; Jori, G.; Kessel, D.; Korbelik, M.; Moan, J.; Peng, Q. *J. Natl. Cancer Inst.* **1998**, *90*, 889.
(5) Sessler, J. L.; Hemmi, G.; Mody, T. D.; Murai, T.; Burrell, A.; Young, S. W. *Acc. Chem. Res.* **1994**, *27*, 43.
(6) Hajri, A.; Wack, S.; Meyer, C.; Smith, M. K.; Leberquier, M.; Aprahamian, M. *Photochem. Photobiol.* **2002**, *75*, 140−148.
(7) Van Tenten, Y.; Schuitmaker, H. J.; De Wolf, A.; Willekens, B.; Vrensen, G. F. J. M.; Tassignon, M. J. *Exp. Eye Res.* **2001**, *72*, 41−48.
(8) Rockson, S. G.; Kramer, P.; Razavi, M.; Szuba, A.; Filardo, S.; Adelman, D. C. *Circulation* **2000**, *102*, 2322.
(9) Lambrechts, S. A. G.; Demidova, T. N.; Aalders, M. C. G.; Hasan, T.; Hamblin, M. R. *Photochem. Photobiol. Sci.* **2005**, *4*, 503−509.
(10) Mang, T. S.; Allison, R.; Hewson, G.; Snider, W.; Moskowitz, R. *Cancer J. Sci. Am.* **1998**, *4*, 378.
(11) Young, S. W.; Woodbourn, K. W.; Wright, M. *Photochem. Photobiol.* **1996**, *63*, 892−897.
(12) Mellish, K. J.; Cox, R. D.; Vernon, D. I.; Griffiths, J.; Brown, S. B. *Photochem. Photobiol.* **2002**, *75*, 392.
(13) Detty, M. R.; Merkel, P. B. *J. Am. Chem. Soc.* **1990**, *112*, 3845.
(14) Williamson, L. M.; Cardigan, R.; Prowse, C. V. *Transfusion* **2003**, *43*, 1322.
(15) Gorman, A.; Killoran, J.; O'Shea, C. *J. Am. Chem. Soc.* **2004**, *126*, 10619−10631.
(16) Killoran, J.; Allen, L.; Gallagher, J. F.; Gallagher, W. M.; O'Shea, D. F. *Chem. Commun.* **2002**, 1862−1863.
(17) Szacilowski, K.; Macyk, W.; Drzewiecka-Matuszek, A.; Brindell, M.; Stockhel, G. *Chem. Rev.* **2005**, *105*, 2647−2694.
(18) Buchler, J. W. In *Porphyrins and Metalloporphyrins*; Smith, K. C., Ed.; Elsevier: Amsterdam, 1975.
(19) Petit, L.; Adamo, C.; Russo, N. *J. Phys. Chem. B* **2005**, *109*, 12214−12221.
(20) Quartarolo, A. D.; Russo, N.; Sicilia, E.; Lelj, F. *J. Chem. Theory Comput.* **2007**, *3*, 860−869.
(21) Quartarolo, A. D.; Russo, N.; Sicilia, E. *Chem. Eur. J.* **2006**, *12*, 6797−6803.
(22) Petit, L.; Quartarolo, A. D.; Adamo, C.; Russo, N. *J. Phys. Chem. B* **2006**, *110*, 2398−2404.
(23) Ciofini, I.; Daul, C.; Adamo, C. *J. Phys. Chem. A* **2003**, *107*, 11182.

(24) Weiss, C. *J. Mol. Spectrosc.* **1972**, *44*, 37.
(25) Hasegawa, J.; Ozeki, Y.; Ohkawa, K.; Hada, M.; Nakatsuji, H. *J. Phys. Chem. B* **1998**, *102*, 1320−1326.
(26) Hasegawa, J.; Hada, M.; Nonoguchi, M.; Nakatsuji, H. *Chem. Phys. Lett.* **1996**, *250*, 159.
(27) Ahlrichs, R.; Bar, M.; Haser, M.; Horn, H.; Kolmel, C. Electronic structure calculations on workstation computers: The program system Turbomole. *Chem. Phys. Lett.* **1989**, *162* (3), 165−169.
(28) Adamo, C.; Barone, V. *J. Chem. Phys.* **1999**, *110*, 6158.
(29) Schaefer, A.; Ahlrichs, H. R. *J. Chem. Phys.* **1992**, *97*, 2571.
(30) Perdew, J. P.; Burke, K.; Ernzerhof, M. *Phys. Rev. Lett.* **1996**, *77*, 3865; **1997**, *78*, 1396.
(31) Schaefer, A.; Huber, C.; Ahlrichs, R. *J. Chem. Phys.* **1994**, *100*, 5829.
(32) Klamt, A.; Schuurmann, G. *J. Chem. Soc., Perkin Trans.* **1993**, *2*, 799.
(33) Tomasi, J.; Persico, M. *Chem. Rev.* **1994**, *94*, 2027.
(34) Barone, V.; Cossi, M. *J. Phys. Chem. A* **1998**, *102*, 1995.
(35) Kobayashi, N.; Konami, H. *J. Porphyrins Phthalocyanines* **2001**, *5*, 233−255.
(36) Zhang, X.; Zhang, Y.; Jiang, J. *J. Mol. Struct.* **2004**, *673*, 103−108.
(37) Toyota, K.; Hasegawa, J.; Nakatsuji, H. *J. Phys. Chem. A* **1997**, *101*, 446−451.
(38) Edwards, L.; Gouterman, M. *J. Mol. Spectrosc.* **1970**, *33*, 292−310.
(39) Kobayashi, S.; Nakajima, H.; Ogata, H.; Fukuda, T. *Chem. Eur. J.* **2004**, *10*, 6294−6312.
(40) McKee, V.; Ong, C. C.; Rodley, G. A. *Inorg. Chem.* **1984**, *23*, 4242−4248.
(41) Wong, A.; Ramsey, I.; Xin, M.; Zhehong, G.; Poh, J.; Gang, W. *J. Phys. Chem. A* **2006**, *110*, 10084−10090.
(42) Dorough, G. D.; Miller, J. R. *J. Am. Chem. Soc.* **1952**, *74*, 6106−6108.
(43) Seely, G. R. *J. Chem. Phys.* **1957**, *27* (1), 125−133.
(44) Eisner, U.; Linstead, R. P. *J. Chem. Soc.* **1955**, 3742−3748.
(45) Eisner, U.; Linstead, R. P. *J. Chem. Soc.* **1955**, 3749−3754.
(46) Anderson, J. S.; Bradbrook, E. F.; Cook, A. H.; Linstead, R. P. *J. Am. Chem. Soc.* **1938**, 1151−1156.
(47) Kovshev, E. I. *Zh. Obshch. Khim.* **1972**, *42*, 696.
(48) Cook, A. H.; Linstead, R. P. *J. Chem. Soc.* **1937**, 929−933.
(49) Baerends, E. J.; Ricciardi, G.; Rosa, A.; van Gisbergen, S. J. A. *J. Phys. Chem. A* **2001**, *105*, 3311−3327.
(50) Linnanto, J.; Korppi-Tommola, J. *Phys. Chem. Chem. Phys.* **2006**, *8*, 663−687.
(51) Linnanto, J.; Korppi-Tommola, J. *J. Phys. Chem. A* **2004**, *108*, 5872−5882.
(52) Sundholm, D. *Chem. Phys. Lett.* **2000**, *317*, 392−399.
(53) Baerends, E. J.; Ricciardi, G.; Rosa, A.; van Gisbergen, S. J. A. *Coord. Chem. Rev.* **2002**, *230*, 5−27.